J. Phys. B: At. Mol. Opt. Phys. **41** (2008) 235202 (5pp) doi:10.1088/0953-4075/41/23/235202

Energy and angle differential cross sections for the electron-impact double ionization of helium

M S Pindzola[1], F Robicheaux[1] and J Colgan[2]

[1] Department of Physics, Auburn University, Auburn, AL, USA
[2] Theoretical Division, Los Alamos National Laboratory, Los Alamos, NM, USA

Received 16 September 2008, in final form 27 October 2008
Published 20 November 2008
Online at stacks.iop.org/JPhysB/41/235202

Abstract
Energy and angle differential cross sections for the electron-impact double ionization of helium are calculated using a non-perturbative time-dependent close-coupling method. Collision probabilities are found by the projection of a time-evolved nine-dimensional coordinate space wavefunction onto fully antisymmetric products of spatial and spin functions representing three outgoing Coulomb waves. At an incident energy of 106 eV, we present double energy differential cross sections and pentuple energy and angle differential cross sections. The pentuple energy and angle differential cross sections are found to be in reasonable agreement with the scaled shapes observed in recent (e, 3e) reaction microscope experiments. Integration of the differential cross sections over all energies and angles yields a total ionization cross section that is also in reasonable agreement with absolute crossed-beams experiments.

(Some figures in this article are in colour only in the electronic version)

1. Introduction

Triple photoionization or electron-impact double ionization of an atom results in three continuum electrons moving in the field of a charged core, that is, the quantal Coulomb four-body problem. For slowly moving escaping electrons, the three pairs of repulsive interactions at large distances create a difficult problem for treatment by many-body perturbation theory. Thus, a non-perturbative time-dependent close-coupling (TDCC) method was developed to treat the quantal Coulomb four-body problem. For the triple photoionization of the Li atom, TDCC total cross sections [1] are in good agreement with synchrotron experiments [2], while for the triple photoionization of the Be atom, TDCC total cross sections [3] are about a factor of 3 lower than double shake-off model calculations [4]. For the electron-impact double ionization of He, TDCC total cross sections [5, 6] are in good agreement with crossed-beams experiments [7], while for the electron-impact double ionization of H^-, TDCC total cross sections [8] are in good agreement with the more recent of two sets of crossed-beams experiments [9, 10].

Recently reaction microscope experiments [11, 12] have provided energy and angle differential cross sections for the electron-impact double ionization of helium. The experimental differential cross sections were found to be in good agreement with three-body Coulomb [13] and convergent close-coupling [14] scaled calculations. In this paper, we extend the time-dependent close-coupling method to calculate energy and angle differential cross sections for the electron-impact double ionization of atoms. We build on previous TDCC calculations of the energy differential cross section for the triple photoionization of the Li atom [15]. Using our new TDCC formulations for energy and angle differential cross sections, we then carry out double energy differential and pentuple energy and angle differential cross section calculations for helium at an incident electron energy of 106 eV. Comparisons are then made with the recent reaction microscope experimental results. The new extension of the TDCC method is presented in section 2, differential cross sections for helium are presented in section 3 and a brief summary is found in section 4. Unless otherwise stated, all quantities are given in atomic units.

2. Theory

The time-dependent close-coupling theory for the electron-impact single and double ionization of an atom has been set

forth in our original work on helium [5]. For electron-impact ionization of an atom with two active electrons, the angular reduction of the time-dependent Schrödinger equation in nine spatial dimensions yields an $l_1 l_2 L l_3$ set of time-dependent coupled partial differential equations given by

$$\mathrm{i}\frac{\partial P^{\mathcal{LS}}_{l_1 l_2 L l_3}(r_1,r_2,r_3,t)}{\partial t} = \sum_{i=1}^{3} T_{l_i}(r_i)\, P^{\mathcal{LS}}_{l_1 l_2 L l_3}(r_1,r_2,r_3,t) + \sum_{l_1',l_2',L',l_3'} \sum_{i<j=1}^{3} V^{\mathcal{L}}_{l_1 l_2 L l_3, l_1' l_2' L' l_3'}(r_i,r_j)\, P^{\mathcal{LS}}_{l_1' l_2' L' l_3'}(r_1,r_2,r_3,t) \tag{1}$$

for each total $\mathcal{LS}$ scattering symmetry. For helium, the one-electron operator, T, is given by

$$T_l(r) = -\frac{1}{2}\frac{\partial^2}{\partial r^2} + \frac{l(l+1)}{2r^2} - \frac{Z}{r}, \tag{2}$$

where $Z = 2$. The two-electron operator, V, contains the three pairs of Coulomb repulsion operators between the two active target electrons and the incident electron.

For scattering from the ground state of helium, the initial time TDCC solutions are given by

$$P^{\mathcal{L}^{\frac{1}{2}}}_{l_1 l_2 L l_3}(r_1,r_2,r_3,t=0) = \delta_{l_1,l}\delta_{l_2,l}\delta_{L,0}\hat{P}_{ll}(r_1,r_2)\delta_{l_3,\mathcal{L}} G_{k_0\mathcal{L}}(r_3), \tag{3}$$

where $\sum_l \hat{P}_{ll}(r_1,r_2)$ is a correlated radial wavefunction for the two target electrons of the ground state of helium, $G_{k_0\mathcal{L}}(r)$ is a Gaussian radial wavepacket for the incident electron and k_0 is the incident electron linear momentum. The final time TDCC solutions,

$$P^{\mathcal{LS}}_{l_1 l_2 L l_3}(r_1,r_2,r_3,t\to\infty), \tag{4}$$

are found by the evolution of equation (1) to sufficiently long times so that distinct Coulomb waves move in the long-range field of the nuclear core.

Projection of the final time TDCC solutions onto fully antisymmetric products of one-electron spin orbitals yields double ionization momentum space probability functions given by

$$\bar{P}^{\mathcal{LS}}_{l_1 l_2 L S l_3}(k_1,k_2,k_3) = \sum_{L',S'}\sum_{ijk}^{6} Q^{\mathcal{LS}}_{l_1 l_2 L S l_3 L' S'}(ijk) \times \int_0^\infty \mathrm{d}r_1 \int_0^\infty \mathrm{d}r_2 \int_0^\infty \mathrm{d}r_3\, P_{k_1 l_1}(r_i) P_{k_2 l_2}(r_j) P_{k_3 l_3}(r_k) \times P^{\mathcal{LS}}_{l_1 l_2 L' l_3}(r_1,r_2,r_3,t\to\infty), \tag{5}$$

where the one-electron radial continuum orbitals, $P_{kl}(r)$, are solutions of the radial Schrödinger equation with a one-electron Hamiltonian operator $T_l(r)$ and ijk is summed over the six permutations of 123. The probability expansion coefficients, Q, are obtained using standard algebraic reduction methods. For scattering from the ground state of helium, for example:

$$Q^{\mathcal{L}^{\frac{1}{2}}}_{l_1 l_2 L S l_3 L' 0}(132) = -\sqrt{\frac{2}{3}}\delta_{S,1}(-1)^{l_2+l_3+L+L'}\sqrt{(2L+1)(2L'+1)}\begin{Bmatrix} l_2 & l_1 & L \\ l_3 & \mathcal{L} & L' \end{Bmatrix}. \tag{6}$$

The total cross section for electron-impact double ionization of the ground state of helium is given by

$$\sigma = \frac{\pi}{2k_0^2}\sum_{\mathcal{L}} 2(2\mathcal{L}+1) \sum_{l_1,l_2,l_3,L,S} \times \int_0^\infty \mathrm{d}k_1 \int_0^\infty \mathrm{d}k_2 \int_0^\infty \mathrm{d}k_3 \left|\bar{P}^{\mathcal{L}^{\frac{1}{2}}}_{l_1 l_2 L S l_3}(k_1,k_2,k_3)\right|^2. \tag{7}$$

The double energy differential cross section for electron-impact double ionization of the ground state of helium is given by

$$\frac{\mathrm{d}^2\sigma}{\mathrm{d}\alpha\mathrm{d}\beta} = \frac{\pi}{2k_0^2}\sum_{\mathcal{L}} 2(2\mathcal{L}+1)\int_0^\infty \mathrm{d}k_1 \int_0^\infty \mathrm{d}k_2 \int_0^\infty \mathrm{d}k_2 \times \delta\left(\alpha - \tan^{-1}\left(\frac{k_2}{k_1}\right)\right)\delta\left(\beta - \tan^{-1}\left(\frac{k_3}{\sqrt{k_1^2+k_2^2}}\right)\right) \times \sum_{l_1,l_2,l_3,L,S}\frac{1}{6}\sum_{ijk}^{6}\left|\bar{P}^{\mathcal{L}^{\frac{1}{2}}}_{l_1 l_2 L S l_3}(k_i,k_j,k_k)\right|^2, \tag{8}$$

where α is an angle in the (k_1,k_2) hyperspherical plane and β is an angle in the plane perpendicular to the (k_1,k_2) hyperspherical plane, both defined from 0 to $\frac{\pi}{2}$.

The pentuple energy and angle differential cross sections for electron-impact double ionization of the ground state of helium are given by

$$\frac{\mathrm{d}^5\sigma}{\mathrm{d}\alpha\,\mathrm{d}\beta\,\mathrm{d}\Omega_1\,\mathrm{d}\Omega_2\,\mathrm{d}\Omega_3} = \frac{\pi}{2k_0^2}\int_0^\infty \mathrm{d}k_1 \int_0^\infty \mathrm{d}k_2 \int_0^\infty \mathrm{d}k_2\,\delta\left(\alpha - \tan^{-1}\left(\frac{k_2}{k_1}\right)\right) \times\delta\left(\beta - \tan^{-1}\left(\frac{k_3}{\sqrt{k_1^2+k_2^2}}\right)\right)\sum_S\frac{1}{6}\sum_{ijk}^{6} \times \left|\sum_{\mathcal{L}} i^{\mathcal{L}}\sqrt{2(2\mathcal{L}+1)}\sum_{l_1,l_2,l_3,L}(-\mathrm{i})^{l_1+l_2+l_3}\,\mathrm{e}^{\mathrm{i}(\delta_{l_1}+\delta_{l_2}+\delta_{l_3})} \times \bar{P}^{\mathcal{L}^{\frac{1}{2}}}_{l_1 l_2 L S l_3}(k_i,k_j,k_k) Y_{l_1 l_2 L l_3 \mathcal{L}}(\Omega_1,\Omega_2,\Omega_3)\right|^2, \tag{9}$$

where δ_l is a Coulomb phase shift and Y is a coupled product of three spherical harmonics.

The integrals over linear momenta k_i found in equations (7)–(9) for the various cross sections are restricted so that the conservation of energy,

$$E_{\mathrm{atom}} + \frac{k_0^2}{2} = \frac{k_1^2}{2} + \frac{k_2^2}{2} + \frac{k_3^2}{2}, \tag{10}$$

is approximately conserved. This has been found to reduce the contamination from the continuum piece of two-electron bound-state wavefunctions. Since the momentum space probabilities, $\bar{P}$, are obtained by projection onto antisymmetric product states, permutation sums are found in both equations (8) and (9) for the differential cross sections. We note that differential cross sections in ejected energies $E_2 = \frac{k_2^2}{2}$ and $E_3 = \frac{k_3^2}{2}$ are given by

$$\frac{\mathrm{d}^2\sigma}{\mathrm{d}E_2\,\mathrm{d}E_3} = \frac{1}{k_1 k_2 k_3\sqrt{k_1^2+k_2^2}}\frac{\mathrm{d}^2\sigma}{\mathrm{d}\alpha\,\mathrm{d}\beta} \tag{11}$$

Table 1. Total partial cross sections for the electron-impact double ionization of helium at low incident energies (1.0 kb = 1.0×10^{-21} cm^2).

$\mathcal{LS}$ symmetry	$l_1 l_2 L l_3$ channels	$(192)^3$ lattice σ(kb) at 100 eV	$l_1 l_2 L l_3$ channels	$(384)^3$ lattice σ(kb) at 100 eV	$(384)^3$ lattice σ(kb) at 106 eV
^{2}S	11	0.14	11	0.08	0.16
^{2}P	21	1.63	21	1.05	1.60
^{2}D	23	2.88	23	1.85	2.93
^{2}F	49	2.38	49	1.43	2.48
^{2}G	63	3.09	60	1.85	3.13
^{2}H	87	0.79	81	0.44	0.92

and

$$\frac{\mathrm{d}^5\sigma}{\mathrm{d}E_2\,\mathrm{d}E_3\,\mathrm{d}\Omega_1\,\mathrm{d}\Omega_2\,\mathrm{d}\Omega_3} = \frac{1}{k_1 k_2 k_3\sqrt{k_1^2+k_2^2}}\,\frac{\mathrm{d}^5\sigma}{\mathrm{d}\alpha\,\mathrm{d}\beta\,\mathrm{d}\Omega_1\,\mathrm{d}\Omega_2\,\mathrm{d}\Omega_3}. \tag{12}$$

3. Results

Standard numerical methods on massively parallel computers are used to solve equation (1) for the coupled radial wavefunctions $P^{\mathcal{LS}}_{l_1 l_2 L l_3}(r_1, r_2, r_3, t)$ and to solve equation (5) for the momentum space probability functions $\tilde{P}^{\mathcal{LS}}_{l_1 l_2 L S l_3}(k_1, k_2, k_3)$. In previous work, we employed both a $(192)^3$ point lattice with a uniform mesh spacing of $\Delta r = 0.20$ [5] and a $(384)^3$ point lattice with a uniform mesh spacing of $\Delta r = 0.10$ [6] to calculate the total double ionization cross section of helium using equation (7) at a number of different incident energies. In this work we employ the same $(384)^3$ point lattice to calculate the total double ionization cross section at an incident energy of 106 eV. The smaller mesh spacing in the $(384)^3$ point lattice gives a better representation of high momentum continuum electrons.

We compare the total partial cross sections from each lattice calculation at low incident energies in table 1. For the $(192)^3$ point lattice, the $\mathcal{L} = 0$–5 total cross section of 10.9 kb at 100 eV was extrapolated [5] in $\mathcal{L}$ to 12.3 kb and compared with absolute crossed-beams measurements [7] of 17.2 kb ± 2.5 kb. Further lattice calculations at incident energies of 150 eV and 200 eV reported in [5] extrapolated total cross sections within the error bars of experiment [7]. Using the $(384)^3$ point lattice, total cross sections were reported [6] at 50 eV intervals from 100 eV to 400 eV. Although the $(384)^3$ point lattice calculations were considerably lower than the $(192)^3$ point lattice calculations, they did track the crossed-beams measurements through the peak of the total double ionization cross section around 300 eV incident energy. Comparing the $(384)^3$ point lattice calculations at 100 eV and 106 eV, we note a sharp increase in all the partial cross sections due to the rapid climb of the total ionization cross section in the energy region from its threshold at 79 eV to its peak at around 300 eV. Since the $(192)^3$ point lattice calculations at 100 eV and the $(384)^3$ point lattice calculations at 100 eV and 106 eV all found a sharp decrease in the partial cross sections going from $\mathcal{L} = 4$ to $\mathcal{L} = 5$, we did not include the $\mathcal{L} = 5$ contributions in our energy and angle differential cross sections.

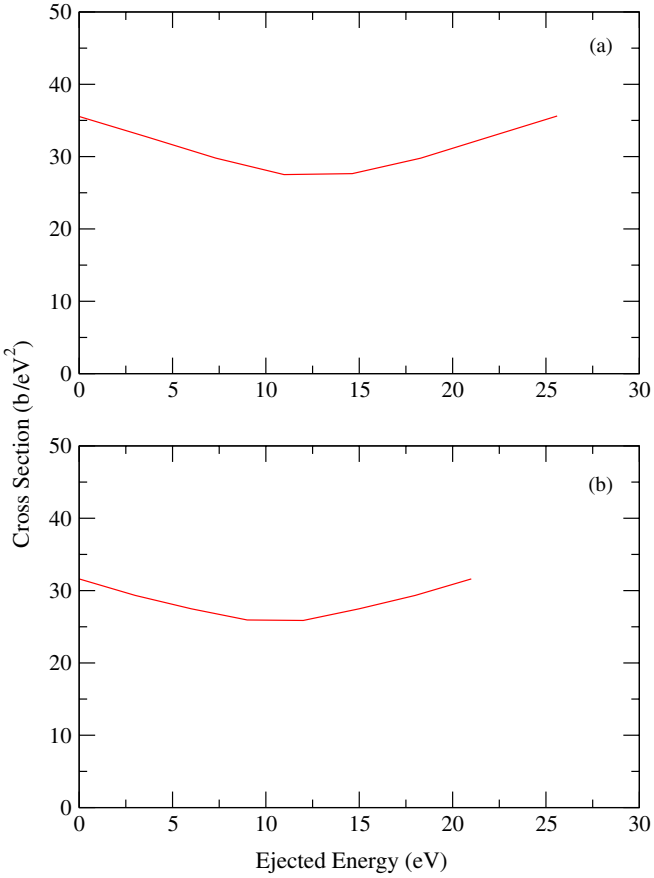

Figure 1. Double energy differential cross sections for the electron-impact double ionization of helium at an incident electron energy of 106 eV. (a) $E_2 = 1.4$ eV and (b) $E_2 = 6.0$ eV (1.0 b = 1.0×10^{-24} cm^2).

Double energy differential cross sections are calculated using equations (8) and (11) at an incident energy of 106 eV. We include partial wave contributions from $\mathcal{L} = 0$–4 with ejected energies ranging from 0.0 eV to 27.0 eV. Using equation (10) we fix $E_2 = \frac{k_2^2}{2}$, vary $E_3 = \frac{k_3^2}{2}$, with $E_1 = \frac{k_1^2}{2}$ determined from knowing $E_{\mathrm{atom}} = -79$ eV and $E = \frac{k_0^2}{2} = 106$ eV. Double energy differential cross sections for $E_2 = 1.4$ eV and 6.0 eV, with variable E_3, are shown in figure 1. The characteristic 'smile' is found for all ejected energies E_2, with the 'smile' becoming shorter and flatter for larger E_2. We note that at equal energy sharing for $E_1 = E_2 = E_3 = 9.0$ eV, the double energy differential cross section is 25 b eV^{-2}.

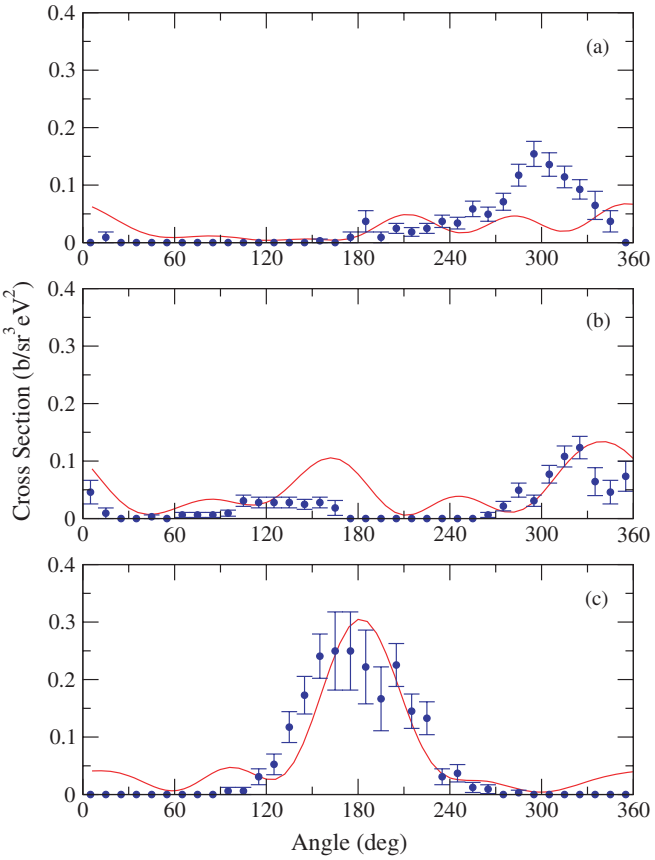

Figure 2. Pentuple energy and angle differential cross sections for the electron-impact double ionization of helium at an incident electron energy of 106 eV. (a) $E_2 = E_3 = 9.0$ eV, $\theta_1 = 45°$, $\theta_2 = 135°$, (b) $E_2 = E_3 = 9.0$ eV, $\theta_1 = 45°$, $\theta_2 = 225°$ and (c) $E_2 = E_3 = 9.0$ eV, $\theta_1 = 45°$, $\theta_2 = 315°$. Solid circles with error bars: reaction microscope measurements [11] divided by a factor of 25 (1.0 b = 1.0×10^{-24} cm^2).

Pentuple energy and angle differential cross sections are calculated using equations (9) and (12) at an incident energy of 106 eV. We include partial wave contributions for $\mathcal{L} = 0$–4 at ejected energies of $E_1 = E_2 = E_3 = 9.0$ eV. Pentuple energy and angle differential cross sections for $\phi_1 = \phi_2 = \phi_3 = 0$, $\theta_1 = 45°, \theta_2 = 135, 225, 315°$ and variable θ_3 are shown in figure 2. The main peaks in the differential cross sections occur when the third ejected electron angle is as far away as possible from the other two ejected electron angles θ_1 and θ_2. Minima in the differential cross sections occur when the third ejected electron angle equals either of the two ejected electron angles θ_1 and θ_2. We compare with recent (e, 3e) reaction microscope measurements [11] at 106 eV for equal energy sharing at the same θ_i angles for a co-planar geometry ($\phi_i = 0$). The measurements have been divided by a factor of 25. The best relative agreement between theory and experiment is found in figure 3(c) for $\theta_2 = 315°$, where the largest cross section is found for $\theta_3 = 180°$, yet is only 0.3 b sr^{-3} eV^{-2}. We expect that further improvement in the relative agreement may come from the inclusion of more $l_1 l_2 L l_3$ coupled channels and $l_1 l_2 L S l_3$ probability projections in the current $\mathcal{L} = 0$–4 lattice calculations, and in the inclusion of higher $\mathcal{LS}$ symmetries. Detailed shapes in the angle differential cross sections are much more slowly convergent than magnitudes of total and energy differential cross sections.

As a check on the absolute magnitude of our differential cross sections, we numerically integrated equation (9) over all hyperspherical (α, β) and regular spherical (θ_i, ϕ_i) angles:

$$\sigma = \int_0^{\frac{\pi}{2}} \mathrm{d}\alpha \int_0^{\frac{\pi}{2}} \mathrm{d}\beta \int_0^{2\pi} \mathrm{d}\phi_1 \int_0^{\pi} \sin(\theta_1)\,\mathrm{d}\theta_1 \int_0^{2\pi} \mathrm{d}\phi_2 \int_0^{\pi} \times \sin(\theta_2)\,\mathrm{d}\theta_2 \int_0^{2\pi} \mathrm{d}\phi_3 \int_0^{\pi} \sin(\theta_3)\mathrm{d}\theta_3 \frac{\mathrm{d}^5\sigma}{\mathrm{d}\alpha\,\mathrm{d}\beta\,\mathrm{d}\Omega_1\,\mathrm{d}\Omega_2\,\mathrm{d}\Omega_3}. \quad (13)$$

The ϕ_i angles were partitioned over all the processors on a massively parallel computer. After lengthy computations, our integrated differential cross sections were found to agree reasonably well with total cross sections obtained directly from equation (7). For example, using a rather crude mesh containing only 78 125 000 points, we obtain a total cross section for the ^{2}P symmetry of 1.33 kb, which compares reasonably well with the 1.60 kb cross section found in the second row and sixth column of table 1. We note that previous comparisons of three-body Coulomb and converged close-coupling calculations with the reaction microscope differential cross section measurements used theory multiplication factors of up to 40 [11].

4. Summary

In conclusion, we have extended a time-dependent close-coupling method for calculating energy and angle differential cross sections for the electron-impact double ionization of atoms. The new TDCC formulation was then applied to calculate double energy differential and pentuple energy and angle differential cross sections for electron-impact double ionization of helium at an incident energy of 106 eV. For equal energy sharing among the three emerging electrons, co-planar pentuple energy and angle differential cross sections were found to be in reasonable agreement with the scaled shapes observed in recent (e, 3e) reaction microscope experiments [11], especially for the largest cross sections at $\theta_1 = 45°$ and $\theta_2 = 315°$. Additional integration checks on the TDCC differential cross sections indicate that their absolute magnitudes should be fairly good.

In the future, we plan to continue convergence studies in lattice size and number of coupled channels, probability projections and total $\mathcal{LS}$ symmetries for the electron-impact double ionization of helium at the current 27 eV excess energy. As the lattice size increases the use of Coulomb waves for projection states becomes more accurate. With an increase in the number of coupled channels and total $\mathcal{LS}$ symmetries the various relative shapes in the angle differential cross sections become more accurate. The TDCC calculations required in support of reaction microscope experiments [16] for the electron-impact double ionization of helium at 5 eV excess energy will be computationally even more challenging. We also plan to continue our studies of the quantal Coulomb four-body problem with large scale numerical calculations of differential cross sections for the triple photoionization of

lithium and electron-impact double ionization of two valence electron atoms, such as beryllium.

Acknowledgments

We would like to thank Alexander Dorn of the MPI in Heidelberg, Germany, for a very useful correspondence. This work was supported in part by grants from the US Department of Energy to Auburn University and Los Alamos National Laboratory. Computational work was carried out at the National Energy Research Scientific Computing Center in Oakland, California and at the National Center for Computational Sciences in Oak Ridge, Tennessee.

References

[1] Colgan J, Pindzola M S and Robicheaux F 2004 *Phys. Rev. Lett.* **93** 053201
[2] Wehlitz R, Huang M T, DePaola B D, Levin J C, Sellin I A, Nagata T, Cooper J W and Azuma Y 1998 *Phys. Rev. Lett.* **81** 1813
[3] Colgan J, Pindzola M S and Robicheaux F 2005 *Phys. Rev.* A **72** 022727
[4] Kheifets A S and Bray I 2003 *J. Phys. B: At. Mol. Opt. Phys.* **36** L211
[5] Pindzola M S, Robicheaux F, Colgan J, Witthoeft M C and Ludlow J A 2004 *Phys. Rev.* A **70** 032705
[6] Pindzola M S, Robicheaux F and Colgan J 2007 *Phys. Rev.* A **76** 024704
[7] Shah M B, Elliott D S, McCallion P and Gilbody H B 1988 *J. Phys. B: At. Mol. Opt. Phys.* **21** 2751
[8] Pindzola M S, Robicheaux F and Colgan J 2006 *J. Phys. B: At. Mol. Opt. Phys.* **39** L127
[9] Peart B, Walton D S and Dolder K T 1971 *J. Phys. B: At. Mol. Phys.* **4** 88
[10] Yu D, Rachafi S, Jureta J and Defrance P 1992 *J. Phys. B: At. Mol. Opt. Phys.* **25** 4593
[11] Durr M, Dorn A, Ullrich J, Cao S P, Czasch A, Kheifets A S, Gotz J R and Briggs J S 2007 *Phys. Rev. Lett.* **98** 193201
[12] Cao S P, Ma X, Dorn A, Durr M and Ullrich J 2008 *Phys. Rev.* A **77** 062703
[13] Gotz J R, Walter M and Briggs J S 2006 *J. Phys. B: At. Mol. Opt. Phys.* **39** 4365
[14] Kheifets A S 2004 *Phys. Rev.* A **69** 032712
[15] Colgan J and Pindzola M S 2006 *J. Phys. B: At. Mol. Opt. Phys.* **39** 1879
[16] Ren X, Dorn A and Ullrich J 2008 *Phys. Rev. Lett.* **101** 093201